Applied Surface Science 256 (2010) 4930–4933

Contents lists available at ScienceDirect

Applied Surface Science

journal homepage: www.elsevier.com/locate/apsusc

Water condensation on zinc surfaces treated by chemical bath deposition

R.D. Narhe[a,b], Wenceslao González-Viñas[a,*], D.A. Beysens[b,c]

[a] Departamento de Física y Matemática Aplicada, Facultad de Ciencias, Universidad de Navarra, c/Irunlarrea s/n 31080, Pamplona, Spain
[b] ESPCI – PMMH, CEA-ESEME, 10 rue Vauquelin, 75231 Paris Cedex 05, France
[c] ESEME, Service des Basses Températures, CEA-Grenoble, Grenoble, France

ARTICLE INFO

Article history:
Received 1 December 2009
Received in revised form 1 March 2010
Accepted 1 March 2010
Available online 7 March 2010

Keywords:
Superhydrophobic surface
Condensation
Coalescence
Chemical bath deposition
Corrosion

ABSTRACT

Water condensation, a complex and challenging process, is investigated on a metallic (Zn) surface, regularly used as anticorrosive surface. The Zn surface is coated with hydroxide zinc carbonate by chemical bath deposition, a very simple, low-cost and easily applicable process. As the deposition time increases, the surface roughness augments and the contact angle with water can be varied from 75° to 150°, corresponding to changing the surface properties from hydrophobic to ultrahydrophobic and superhydrophobic. During the condensation process, the droplet growth laws and surface coverage are found similar to what is found on smooth surfaces, with a transition from Cassie-Baxter to Wenzel wetting states at long times. In particular, it is noticeable in view of corrosion effects that the water surface coverage remains on order of 55%.

1. Introduction

Wettability of liquid on solid is extremely important in our daily life and also in industry and agriculture. One can cite, for instance, the cases of wetting of water on glass windows, painting on different kinds of surfaces and spreading of pesticide on plants. In the wetting process, the chemical composition and the geometric structure of the surface play a key role. Completely wetting surfaces are frequently used in antifogging windows or bacteria resistance coating [1] while extremely non-wetting surfaces (i.e. superhydrophobic surfaces where the contact angle is larger than 150°) are mostly used in self-cleaning surfaces [2], tunable lenses [3], micro-fluidic systems [4] and non-adhesive coating [5,6]. Since the last two decades, the wetting phenomena on superhydrophobic surface has become a subject of fundamental research in physics [7–9], chemistry [10], biology [11,12] and materials science [13,14]. In material science, many metallic superhydrophobic surfaces are mostly used as anticorrosive surfaces. In particular, zinc and zinc oxide surfaces are particularly interesting because of their special electrical, optical and switchable wetting properties.

Superhydrophobic surfaces are in principle rough surfaces. A water drop deposited on such surfaces can rest in a Wenzel state [15] or a Cassie-Baxter state [16], the selection depending on the most stable situation. In the Wenzel state, water fills the microstructure and the apparent contact angle θ^* of a deposited drop is given by

$$\cos\theta^* = r\cos\theta. \quad (1)$$

Here r is the surface roughness defined as the ratio of the actual surface area to the projected surface area and θ is the equilibrium contact angle. In the Cassie-Baxter state, the rough surface is composed of solid and air. A water drop sits partially on the solid surface and partially on the air trapped in the microstructure. In such a situation, the apparent contact angle θ^* is given by

$$\cos\theta^* = \phi_s[\cos\theta + 1] - 1. \quad (2)$$

The angle θ^* depends on the area fraction of the liquid–solid interface (Φ_s), the liquid–air interface ($1-\Phi_s$) and θ. For a given set of r, θ, and Φ_s values, the equilibrium state of the drop will depend on whether the minimum energy corresponds to a Wenzel or a Cassie-Baxter type. The critical contact angle of a drop that determines the wetting situation is given by [17]

$$\theta_c = \cos^{-1}[(\phi_s - 1)/(r - \phi_s)]. \quad (3)$$

When $\theta > \theta_c$, the most stable state is of Cassie-Baxter type; when $\theta < \theta_c$, the most stable state is of Wenzel type. Furthermore, a transition from a high energy state to a low energy state is always possible if the drop gained the required energy to overcome the transition barrier (e.g. by pushing a deposited drop with a syringe to go from a Cassie-Baxter type to a Wenzel type).

Numerous correlations between superhydrophobic surface configurations and liquid wetting properties in case of deposited (projected) drops have been reported in many experimental and theoretical studies. In contrast, and although this process is of

* Corresponding author. Tel.: +34 948425600x6385; fax: +34 948425649.
E-mail address: wens@fisica.unav.es (W. González-Viñas).

0169-4332/$ – see front matter © 2010 Elsevier B.V. All rights reserved.
doi:10.1016/j.apsusc.2010.03.004

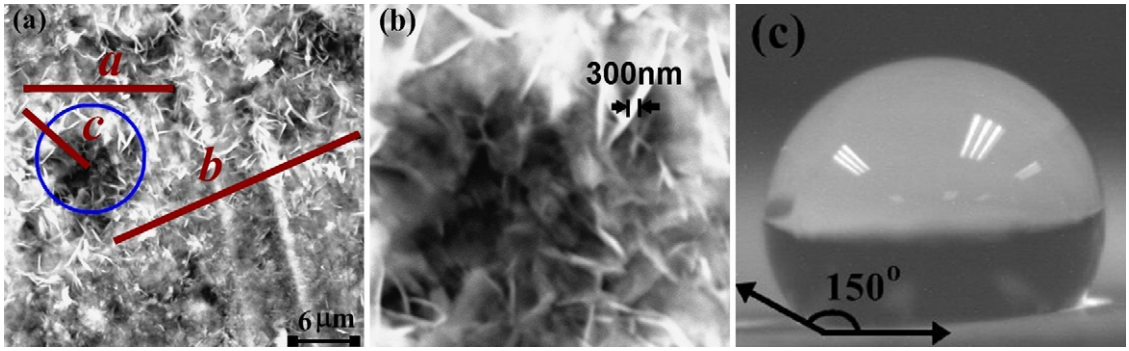

Fig. 1. (a) Scanning electron microscope images of zinc surface (24 h deposition) showing micro-flowers-like structure on the surface (size, $a \approx 12\,\mu m$; separation, $b \approx 25\,\mu m$; height $c \approx 10\,\mu m$). (b) The micro-flower area inside the circle in (a) at large magnification. It shows nano sheets with average thickness 300 nm. (c) Contact angle measurement of a 3 μl water drop on the same surface.

major importance for the evaluation of corrosion, the studies of condensation-induced wetting on superhydrophobic surface and their corresponding wetting properties (self-cleanliness, different wetting states), are much less documented [18–29]. The aim of the present work is thus to study condensation of water on a multi-scale rough superhydrophobic surface where the contact angle is varied in a wide range (70–150°).

2. Experimental

In the present study, we use a zinc substrate whose surface wetting properties can be easily tuned. A plain zinc surface is hydrophobic and, when coated with hydroxide zinc carbonate (HZC) by chemical bath deposition, depending on the deposition time, it can become either ultra hydrophobic or superhydrophobic. The substrate that we used is a 1 mm thick zinc sheet (99.97%). The zinc substrate is provided by Goodfellow (U.K). Analytical grade N-N-dimethylformamide (C_3H_7NO) (DMF) is supplied by Panreac Química S.A.U. (Spain) and urea $(NH_2)_2CO$ is supplied by Merck KGaA (Germany). They are used as it is supplied. We follow the similar method as reported in [30] to modify the contact angle of the substrate by chemical bath deposition. This process is very simple, low-cost and easily applicable. In brief, a small piece of zinc substrate (1.0 cm × 1.5 cm) is immersed in a 2 M urea solution prepared with deionized water and N-N-dimethylformamide (DMF) in 2:1 (v/v) ratio, in sealed bottle and kept at 80 °C for 20–24 h. The substrates were then rinsed for several times with deionized water and dried by dry nitrogen flow. When the zinc substrate is immersed in the 2 M urea solution it changes color from dark silver to gray (off-white) after HZC film deposition. The contact angle is varied by changing the deposition time. The surface morphology is studied with a scanning electron microscope (Zeiss DSM 940A).

Fig. 1(a) shows a typical SEM image of the zinc surface for a 24 h deposition. Micro-bump-like structures (low magnification) and micro-flower-like structures (large magnification) are observed. Furthermore, the flower-like structures are made up of interconnected nano sheets of thickness ranging from 100 to 300 nm (Fig. 1(b)). The average micro-flower sizes are estimated from the scanning electron micrograph: size, $a \approx 12\,\mu m$; separation, $b \approx 25\,\mu m$; height $c \approx 10\,\mu m$. The corresponding average surface roughness is then $r = 1 + 4ac/(a+b)^2 \approx 1.35$ and the area fraction of the liquid–solid interface, $\phi_s = a^2/(a+b)^2 \approx 0.11$. Using these values in Eq. (3), one obtains a critical angle $\theta_c \approx 135°$, larger than the equilibrium contact angle as measured on a flat, non-deposited zinc surface, $\theta = 75 \pm 2°$. This value, taken as the equilibrium value, is the average of the advancing ($\theta_a = 82 \pm 2°$) and receding ($\theta_r = 68 \pm 2°$) contact angle. Although the actual equilibrium contact angle can take any values between θ_a and θ_r, one arbitrarily defined its mean value as $\theta = (\theta_a + \theta_r)/2$. The uncertainty is the measurement uncertainty. The contact angle of water on the substrate is measured by the sessile drop method: a small drop of 3 μl is deposited on the substrate by means of micro-syringe and visualized using a CCD camera with macro lens. Pushing the liquid gives θ_a, pulling it gives θ_r. From the above values $\theta < \theta_c$ and the most stable state is then the Wenzel state. The Wenzel and Cassie-Baxter apparent contact angle are obtained from Eqs. (1) and (2) as $\theta^*_W = 69.5°$ ($\theta^*_{W\,adv} = 79.2°$, $\theta^*_{W\,rec} = 59.6°$) and $\theta^*_{CB} = 149.5°$ ($\theta^*_{CB\,adv} = 151.0°$, $\theta^*_{CB\,rec} = 148.0°$). Both values of θ^*_W and θ^*_{CB} are in good agreement with $\theta^*_W = 70°$ (as obtained from the saturated surface coverage value $\varepsilon^2 \approx 0.65$, see below, Eq. (4)) and $\theta^*_{CB} = 150 \pm 2°$. The latter value has been obtained experimentally by the sessile drop method on the deposited zinc surface, see Fig. 1c, with an advancing contact angle $\theta_a = 155 \pm 2°$ and a receding contract angle $\theta_r = 145 \pm 2°$.

In a condensation experiment a cleaned substrate is fixed on a thick electrolytic copper plate located inside the condensation chamber. Air flow is saturated with water vapor by bubbling into ultra pure water. It is sent to the chamber with a flow rate kept fixed at $0.6\,L\,min^{-1}$ for all experiments. The temperature difference between the saturated water vapor (at room temperature = (23 ± 0.5) °C and the supersaturated vapor (substrate) is (8 ± 0.5) °C. Heterogeneous dropwise water nucleation takes place on the substrate. The growth of drops is observed with a video camera attached to an optical microscope and recorded on a video recorder. Video images are lately digitized and analyzed by Image Tool software.

3. Results and discussion

During condensation, we observed in general the following growth stages.

Initial stage. At the beginning, typically $t < 3$ min, very small drops nucleate on the rough surface. The atomic composition and hydrophilicity of HZC film contributes to the final surface wettability and hence facilitates the nucleation of the drops [30]. The drop surface coverage ε^2 (ratio of area covered by the drops to the total surface area) is low and only a very few number of drop coalescence takes place. Then the drops grow mainly by direct vapor condensation, the drop volume increases as time t and the drop radius $\langle R \rangle$ grows as $\langle R \rangle \sim t^{1/3}$.

Intermediate stage. Typically $3 < t < 8$ min (Fig. 2(a–d)). The drops condensed on the micro-flower-like surface give an impression of being brighter. This is due to their high surface curvature, corresponding to a large apparent contact angle that shows that they are in a Cassie-Baxter state. The surface coverage increases significantly. These drops, if they do not coalesce, remain in the Cassie-Baxter state. In contrast, drops condensing in the vicinity of flowers appear as dark or black, corresponding to a low apparent

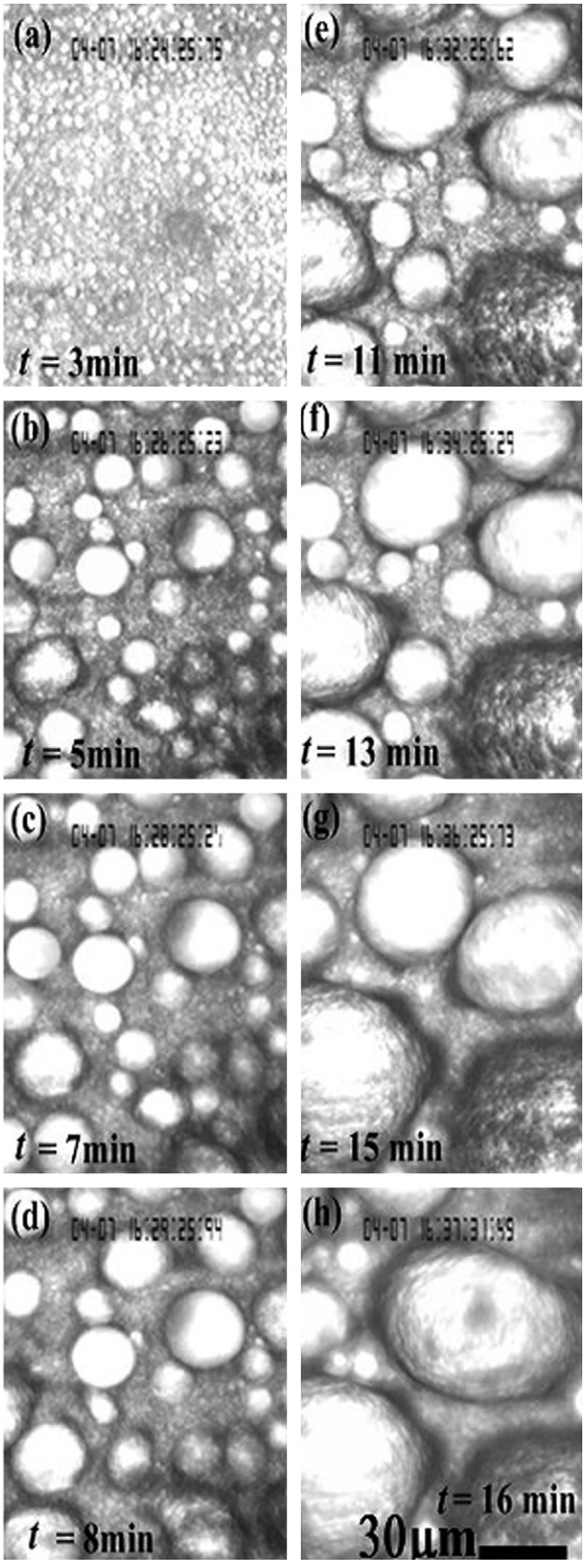

Fig. 2. A typical sequential optical micrograph of condensed water drops on superhydrophobic surface with contact angle $150 \pm 2^{\circ}$.

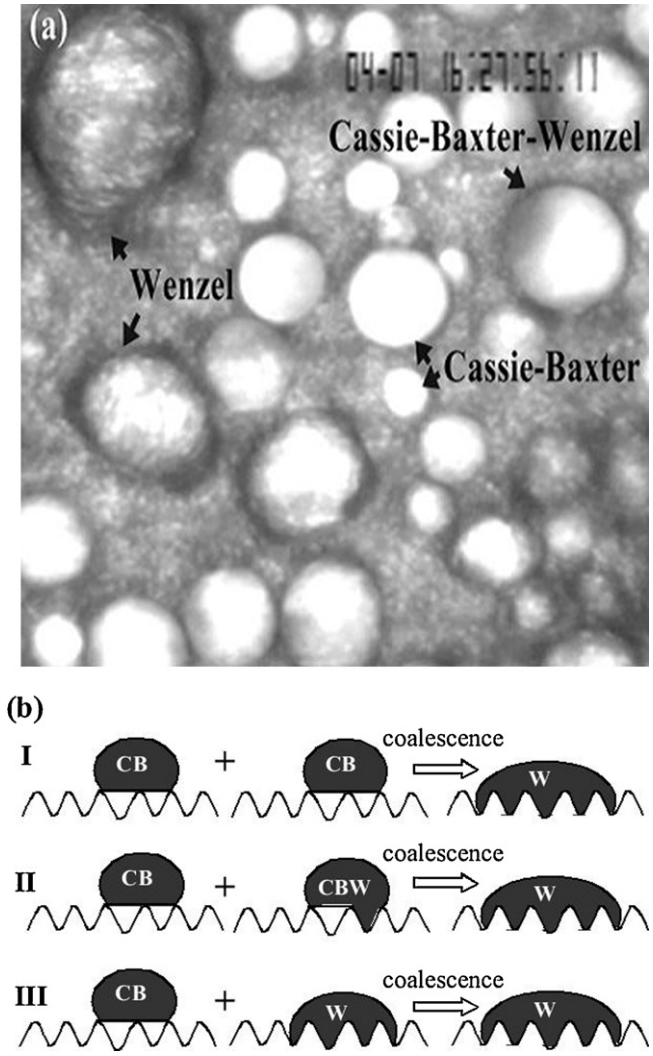

Fig. 3. (a) Three different types of drops Wenzel, Cassie-Baxter, and mixed Cassie-Baxter-Wenzel observed during condensation. (b) Illustration showing the transition of Cassie-Baxter (CB) and Cassie-Baxter -Wenzel (CBW) state to Wenzel (W) state.

contact angle. These drops grow and coalesce as Wenzel type drops. An intermediate mixed Wenzel, Cassie-Baxter case is observed. It corresponds to a drop that is dark on one side and bright on the other side (Fig. 3(a)).

At this stage, three types of drops viz. Wenzel, Cassie-Baxter and mixed, Cassie-Baxter-Wenzel drops (Fig. 3(a)) are then observed. The coalescence of any two types of drop (Cassie-Baxter, Cassie-Baxter-Wenzel, and Wenzel) always results into the expected most stable Wenzel drop (Fig. 3(b)).

The energy gained by drops during coalescence is thus sufficient for inducing the transition from Cassie-Baxter or Cassie-Baxter-Wenzel to the stable Wenzel state. All three types of drops are clearly distinguished when the microscope is precisely focused on one specific drop type. Note that, recently, Boreyko and Chen [29] reported a spontaneous drop removal as a result of surface energy released due to the drop coalescence during condensation. In contrast to our study, those coalescing water drops have large contact angle $\approx 170^{o}$ (as can be estimated from their movie and [22]), hence the pinning forces on the surface of the drop contact line are quite small, making possible spontaneous drop removal. In addition, the critical angle is θ_c ($\approx 94^{o}$) $< \theta$ ($\approx 101^{o}$) [22], which means that the Cassie-Baxter state is the most favorable state. In contrast, in our

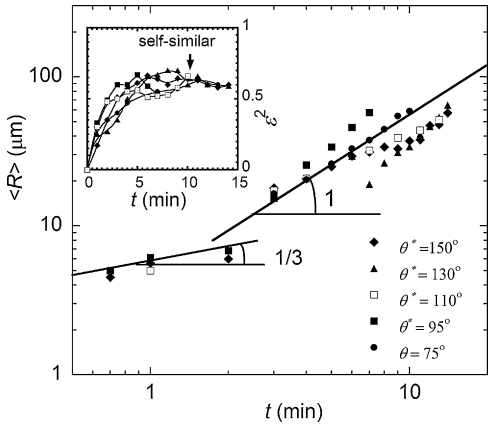

Fig. 4. Evolution of the average drop radius $\langle R\rangle$ on log-log scale for various Cassie-Baxter contact angles (θ^*) on zinc surface corresponding to different deposition times. The straight lines are $t^{1/3}$ and t^1. The inset shows the evolution of the surface coverage (ε^2).

case, the critical angle is θ_c (≈135°) > θ (≈75°), making the Wenzel state the most favorable state.

Late stage. 11 < t < 16 min. Due to drop coalescences and the pinning of the contact line, many non-circular drops are observed on most of the surface. In this stage, due to significant numbers of coalescences events of large drops, the growth law exponent of the mean drop radius $\langle R\rangle$ becomes unity (Fig. 4), which is in agreement with a growth law as $\langle R\rangle \sim t^{1/(D_d-D_s)}$ [32,33]. Here D_d = 3 is the drop dimensionality and D_s = 2 is the surface dimensionality. Boreyko and Chen [29] in the experiment noted above reported a somewhat different growth law exponent 0.74 and 0.82 on hydrophobic and superhydrophobic surfaces, respectively. They consider that these low values are due to experiments performed over a too small time interval. (They also explain the growth exponents lower than the expected value 1/3 in the initial stage [18–20,31,32]) by the initial transient cooling of the cold plate).

The coalescence of Cassie-Baxter and Cassie-Baxter-Wenzel drops with Wenzel drops results into the most stable Wenzel drops. At this stage, the surface coverage saturates around a value that depends on the apparent contact angle according to [33]

$$\varepsilon_\infty^2 = 1 - \frac{\theta}{200}. \quad (4)$$

The surface coverage saturates between 0.62 and 0.65 (Fig. 4 inset). From the saturation surface coverage one can then deduce the mean apparent contact angle θ^*, expected Wenzel. It is found in the range 70–76°, in good agreement with the expected value from Eq. (1), $\theta^*_W \approx 70°$. Contact line pinning also increases the contact angle hysteresis and results into non-circular drops.

Fig. 4 shows the evolution of $\langle R\rangle$ in log-log scales for different contact angles. The different values of contact angles are for different surface wetting properties (i.e. different deposition time). Here $\langle R\rangle$ is the average of the drop radii. For non-circular drops, the larger drop size was considered. As noted just above, drops are indeed very often non-circular. Due to the surface roughness, there is a strong pinning of the contact line in preferred directions and the capillary force is not strong enough to overcome the pinning force. Hence, the coalesced drops are not capable to relax towards its circular equilibrium shape. One notices in Fig. 4 that the average drop radius evolution follows $\langle R\rangle \sim t^{1/3}$ in the initial stage and $\langle R\rangle \sim t^1$ in the late stage, in agreement with the growth of water drops on smooth planar surfaces [32].

4. Concluding remarks

The study of the condensation process on Zn-modified surfaces by chemical bath deposition technique – a very simple and powerful method to modify the surface roughness and wettability, from hydrophobic to superhydrophobic – shows that, on such surfaces, water condensation, although a complex and challenging process, is similar to smooth planar surfaces. As the nucleation events occur at a much smaller length scale than the surface texture scales, the surface chemistry dominates the texture effects during condensation and therefore leads to similar results as on a smooth surface. In particular, it is noticeable in view of corrosion effects that the water surface coverage remains on order of 55%.

Acknowledgments

This work was partly supported by the Spanish MEC (Grant n. FIS2008-01126) and by Departamento de Educación (Gobierno de Navarra). R.D.N. acknowledges the support of Marie Curie International Incoming Fellowship (MCIIF) within the 7th European Community Framework Program. We thank Prof. Jordana for taking SEM images of the substrate.

References

[1] P. Lenz, Adv. Mater. 11 (1999) 1531.
[2] W. Bharthlott, C. Neinhuis, Planta 202 (1997) 1.
[3] S. Kuiper, B.H.W. Hendricks, Appl. Phys. Lett. 85 (2004) 1128.
[4] H. Ghau, S. Herminghaus, P. Lenz, R. Lipowsky, Science 283 (1999) 46.
[5] P. Aussillous, D. Quéré, Nature 411 (2001) 924.
[6] J. Bico, C. Tordeux, D. Quéré, Europhys. Lett. 55 (2001) 214.
[7] M. Caillies, D. Quéré, Soft Matter 1 (2005) 55.
[8] A. Lafuma, D. Quéré, Nat. Mater. 2 (2003) 457.
[9] A. Otten, S. Herminghaus, Langmuir 20 (2004) 2405.
[10] R. Blossey, Nat. Mater. 2 (2003) 301.
[11] X. Hong, X.F. Gao, L. Jaing, J. Am. Chem. Soc. 129 (2007) 1478.
[12] K.Y. Suh, S. Jon, Langmuir 21 (2005) 6836.
[13] X. Zhang, F. Shi, Xi Yu, Haun Liu, Yu Fu, Zhiqiang Wang, Lei Jaing, Xiaoyuan, J. Am. Chem. Soc. 126 (2004) 3064.
[14] Z. Wang, N. Koratkar, L. Ci, P.M. Ajyan, Appl. Phys. Lett. 90 (2007) 143117.
[15] R.N. Wenzel, Ind. Eng. Chem. 28 (1936) 988.
[16] A.B.D. Cassie, S. Baxter, Trans. Faraday Soc. 40 (1944) 546.
[17] B. He, N. Patankar, J. Lee, Langmuir 19 (2003) 4999.
[18] R.D. Narhe, D.A. Beysens, Phys. Rev. Lett. 93 (2004) 076103.
[19] R.D. Narhe, D.A. Beysens, Europhys. Lett. 75 (2006) 98.
[20] R.D. Narhe, D.A. Beysens, Langmuir 23 (2007) 6486.
[21] Y.T. Cheng, D.E. Rodak, Appl. Phys. Lett. 87 (2005) 194112.
[22] C.–H. Chen, Q. Cai, C. Tsai, C.-L. Chen, Appl. Phys. Lett. 90 (2007) 173108.
[23] C. Dorrer, J. Ruhe, Langmuir 23 (2007) 3820.
[24] K.K. Varanasi, Min Hsu, N. Bhate, W. Yang, Tao Deng, Appl. Phys. Lett. 95 (2009) 094101.
[25] Y. Zheng, D. Han, J. Zhai, L. Jiang, Appl. Phys. Lett. 92 (2008) 084106.
[26] X. Xiao, Y.T. Cheng, J. Mater. Res. 23 (2008) 2174.
[27] B. Mockenhaupt, H.J. Ensikat, M. Speath, W. Bharthlott, Langmuir 24 (2008) 13591.
[28] J.B. Boreyko, C.-H. Chen, Phys. Rev. Lett. 103 (2009) 174502.
[29] J.B. Boreyko, C.-H. Chen, Phys. Rev. Lett. 103 (2009) 184501.
[30] Bin Su, Mei Li, Zhengyu Shi, Qinghua Lu, Langmuir 25 (2009) 3640.
[31] J.L. Viovy, D. Beysens, C.M. Knobler, Phys. Rev. A 37 (1988) 4965.
[32] D. Fritter, C.M. Knobler, D. Beysens, Phys. Rev. A 43 (1991) 2858.
[33] H. Zhao, D. Beysens, Langmuir 11 (1995) 627.